Ferritins: Dynamic Management of Biological Iron and Oxygen Chemistry

XIAOFENG LIU AND ELIZABETH C. THEIL*

Center for BioIron at CHORI (Children's Hospital Oakland Research Institute), Oakland, CA 94609

Received June 4, 2004

ABSTRACT

Ferritins are spherical, cage-like proteins with nanocavities formed by multiple polypeptide subunits (four-helix bundles) that manage iron/oxygen chemistry. Catalytic coupling yields diferric oxo/hydroxo complexes at ferroxidase sites in maxi-ferritin subunits (24 subunits, 480 kDa; plants, animals, microorganisms). Oxidation occurs at the cavity surface of mini-ferritins/*Dps* proteins (12 subunits, 240 kDa; bacteria). Oxidation products are concentrated as minerals in the nanocavity for iron−protein cofactor synthesis (maxi-ferritins) or DNA protection (mini-ferritins). The protein cage and nanocavity characterize all ferritins, although amino acid sequences diverge, especially in bacteria. Catalytic oxidation/di-iron coupling *in* the protein cage (maxi-ferritins, 480 kDa; plants, bacteria and animal cell-specific isoforms) or *on* the cavity surface (mini-ferritins/*Dps* proteins, 280 kDa; bacteria) initiates mineralization. Gated pores (eight or four), symmetrically arranged, control iron flow. The multiple ferritin functions combine pore, channelm and catalytic functions in compact protein structures required for life and disease response.

Introduction

Exploiting the energy of iron and oxygen chemistry for biology within the constraints of aqueous environments at neutral pH and moderately low temperature and with few free radicals illustrates the power of the partnership between inorganic and biological chemistries. Central to all iron- and oxygen-dependent cellular activities is a family of spherical protein cages, the ferritins,[1] which mainly use oxygen to concentrate cellular iron. The oxidized ferric ion inside ferritin is a solid under physiological pH, protected by ferritin protein at concentrations $\sim 10^{14}$ higher than aqueous ferric ion concentration. Iron concentrated in ferritin is used to synthesize iron cofactors for respiration, photosynthesis, nitrogen fixation, and DNA synthesis. Ferritins are central to life, as exemplified by increased oxidant sensitivity and the lethality of gene deletion.[2−9] Ferritin mutations affect liver[10] or the central nervous system.[11−13] The control of ferritin synthesis is unusually complex with regulatory steps involving both DNA (transcription) and mRNA (translation).[14,15] New observations that are particularly emphasized relate to flexibility of ferritin proteins.

Ferritins are large protein cages formed by arrays of self-assembling α-helices (24 or 12 four-helix bundles or subunits) with nanocavities (5−8 nm), that catalytically couple iron and oxygen at protein sites for precursors of the cavity mineral. The ferritins are ubiquitous in microorganisms, plants, and animals. DNA and protein sequences for ferritins vary, especially in bacteria, but tertiary/quaternary structures are conserved indicating that the amino acid sequences have the same or similar folding information for the conserved protein cage and nanocavity.

Thousands (up to 4500) of iron atoms can be accommodated in ferritin minerals inside the protein cage. The maxi-ferritins of animals, plants, and bacteria (∼480 kDa, 24 subunits) use oxygen to make the iron concentrates.[16,17] A catalytically inactive subunit form, called L subunit, that is specific to animals, coassembles with catalytically active (H) subunits. In hepatocytes, for example, the L/H ratio is 2:1 compared to a ratio in cardiomycytes of 0.3:1, which may reflect differences in sensitivity to the H_2O_2 byproducts of ferritin catalysis. Mini-ferritins of bacteria and archaea (∼240 kDA, 12 subunits), in contrast to maxi-ferritins where dioxygen is used to concentrate iron, use iron to detoxify dioxygen or peroxide and protect DNA from damage.[3,4,6,7] Mini-ferritins were first discovered during starvation and named *Dps* (DNA protection during starvation) proteins.

The first step in concentrating iron in maxi-ferritins is oxidizing and coupling two ferrous ions via a diferric peroxo (DFP) complex to form diferric oxo complex precursors of the hydrated ferric oxide mineral. The second product is H_2O_2.[16,17] The catalytic ferroxidase site is in the center of the helix bundle of each maxi-ferritin subunit (Figure 1). DFP decay products appear to leave the catalytic site in different directions: diferric oxy-mineral precursors go to the protein cavity and H_2O_2 goes into solution.[18]

The overall and intermediate reactions are shown in eqs 1−4.[19] The catalytic or ferroxidase (F_{ox}) reaction (eq 1 and 2) is fast (milliseconds), although days to months may be required in vivo for the overall reaction (eq 4), since the liquid/solid-phase transitions are slow. When iron concentrations in cells are very high, ferritin also functions as an iron "scavenger"[20] by sequestering "excess" cellular iron. In mini-ferritins, the ferroxidase reaction and site are less well characterized but appear to be able to use either dioxygen or H_2O_2 as substrates.[3]

Xiaofeng Liu received his B.S. degree in Chemistry from Jilin University (China) and Ph.D. in Biochemistry working with Dr. Richard Honzatko, Iowa State University, in 2001. He then worked as a postdoctoral fellow of Dr. Elizabeth C. Theil at Children's Hospital Oakland Research Institute (CHORI), studying animal ferritin structure and function, and is currently a Postdoctoral Scholar at CHORI. He is a recipient of a Cooley's Anemia Foundation Fellowship.

Elizabeth C. Theil, born in New York, NY, received her Ph.D. from Columbia University after receiving a B.S. degree from Cornell. In 1998, she resigned her position as The University Professor of Biochemistry and Physics at North Carolina State University (NCSU) to move her program to CHORI, a private research institute owned by Children's Hospital and Research Center at Oakland. Currently she holds the positions of CHORI Senior Scientist, Professor of Molecular and Structural Biochemistry, NCSU (adj), and Professor of Nutrition and Toxicology, University of California at Berkeley (adj).

* Corresponding author.

10.1021/ar0302336 CCC: $30.25
Published on Web 01/29/2005

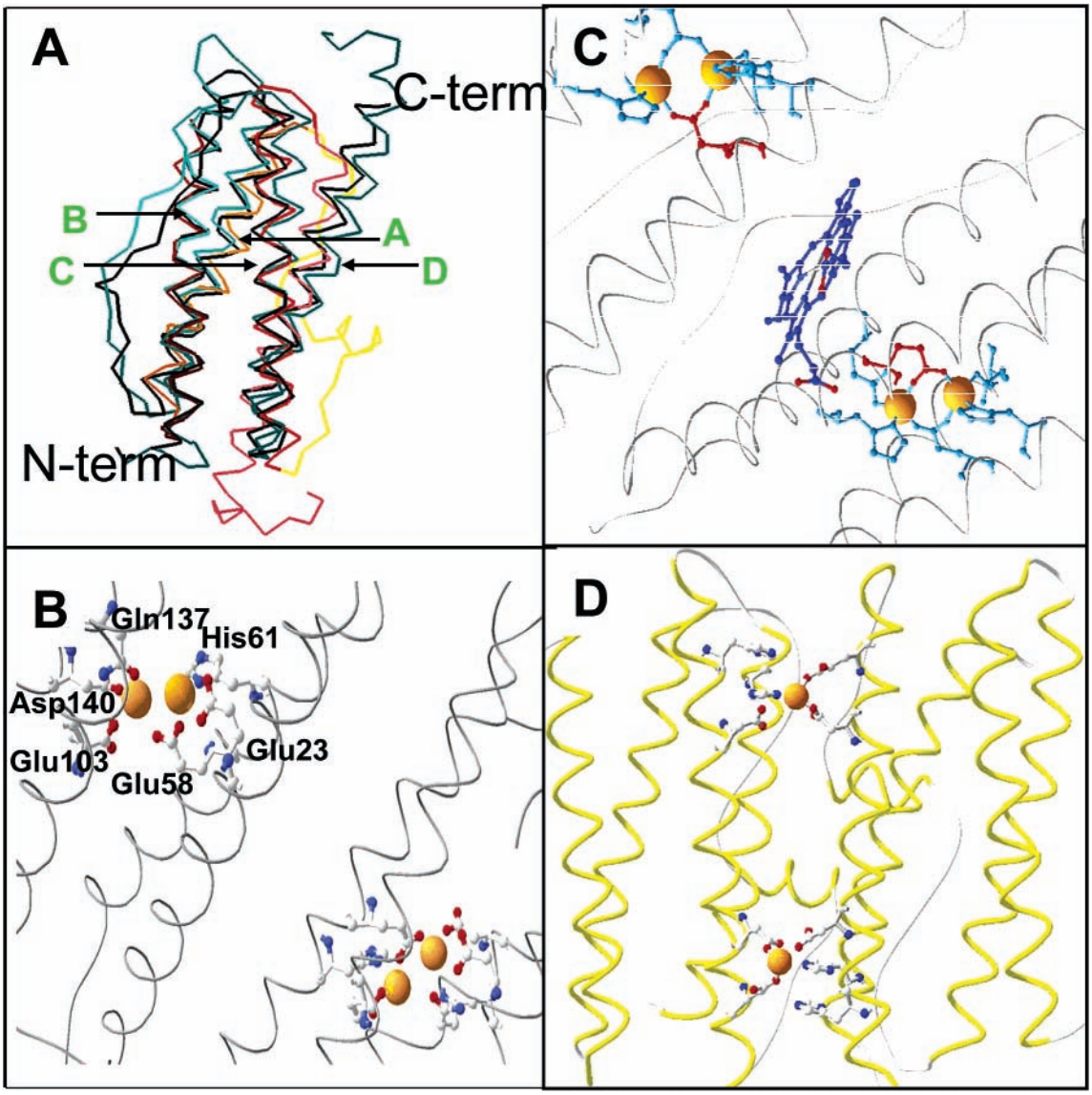

FIGURE 1. Polypeptide helix tetrads and ferroxidase (F_{ox}) sites in maxi-ferritins and mini-ferritins: (A) superposition of helix tetrads that form the subunits of ferritins labeled A, B, C, and D starting from the N-terminus—vertebrate maxi-ferritin (frog M, 1MFR, dark green), *E. coli* bacterioferritin (1BFR, black), and *E. coli Dps* protein (1DPS) where the superposition of four-helix bundles beginning from the N-terminus is reversed (helix A, light red (N-terminus); helix B, red; helix C, yellow; helix D, brown; the A−B (red) and B−C (yellow) loops of the mini-ferritin do not superimpose on the corresponding loops in maxi-ferritins); (B) the F_{ox} site within the four-helix bundles of a single subunit of a vertebrate ferritin (frog M) (all identified amino acids are required to form the diferric peroxo intermediate; ferrous ions are shown as yellow/gold spheres); (C) F_{ox} sites in two subunits of a heme-containing bacterial maxi-ferritin (redrawn from crystal structure of *E. coli* Bfr complexed with Mn (1BFR); heme is in dark blue); (D) F_{ox} sites between two subunits of a mini-ferritin (*E. coli Dps* protein), predicted from *E. coli Dps* protein crystal structure (1DPS).

Maxi-ferritin:

$$2Fe^{2+} + O_2 \rightarrow [Fe(III)-O-O-Fe(III)] \quad (1)$$

$$[Fe(III)-O-O-Fe(III)] + H_2O \rightarrow H_2O_2 + [Fe(III)-O-Fe(III)] \quad (2)$$

$$[Fe(III)-O-Fe(III)] + (H_2O)_{x+2} \rightarrow Fe_2O_3(H_2O)_x + 4H^+ \quad (3)$$

$$2Fe^{2+} + O_2 + (H_2O)_{x+3} \rightarrow Fe_2O_3(H_2O)_x + 4H^+ + H_2O_2 \quad (4)$$

Mini-ferritin:

$$2Fe^{2+} + H_2O_2 + (H_2O)_{x+1} \rightarrow [?] \rightarrow Fe_2O_3(H_2O)_x + 4H^+ \quad (5)$$

The ferroxidase site in maxi-ferritin is a modified di-iron oxygenase site,[21−23] and ferritins are members of the di-iron carboxylate protein family[24] (see Figure 2), which all form DFP intermediates.[18,22,25−31] In ferritins, iron is a substrate with transient binding, contrasting with the di-iron cofactor oxygenases, where iron is a cofactor with stable binding. One of the bacterial maxi-ferritins, Bfr, however, also has canonical di-iron cofactor site ligands and apparently uses small amounts of iron as a cofactor to initiate mineralization of iron without releasing H_2O_2.[32] A common ancestor of ferritin ferroxidase sites and di-iron oxygenases is suggested by the iron ligand similarities and by the simple DNA codon relationships of divergent ligands.[22,23] Ferritin iron is recovered from the ferritin

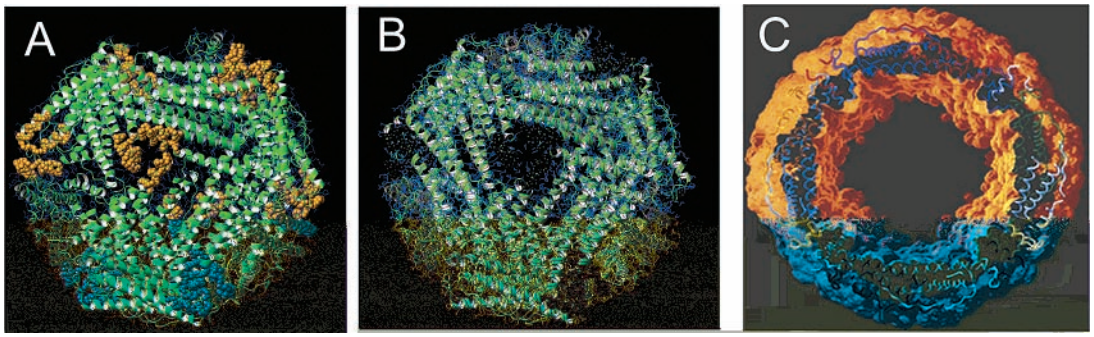

FIGURE 2. Assembled ferritin structures: (A) reproduced with permission from ref 34 (issue cover); copyright 2003 National Academy of Sciences, U.S.A.; (B) ferritin with pores "open" or unfolded; (C) cross-section of an assembled maxi-ferritin showing the nanocavity (reproduced with permission from ref 85; copyright 1994 Wiley Interscience).

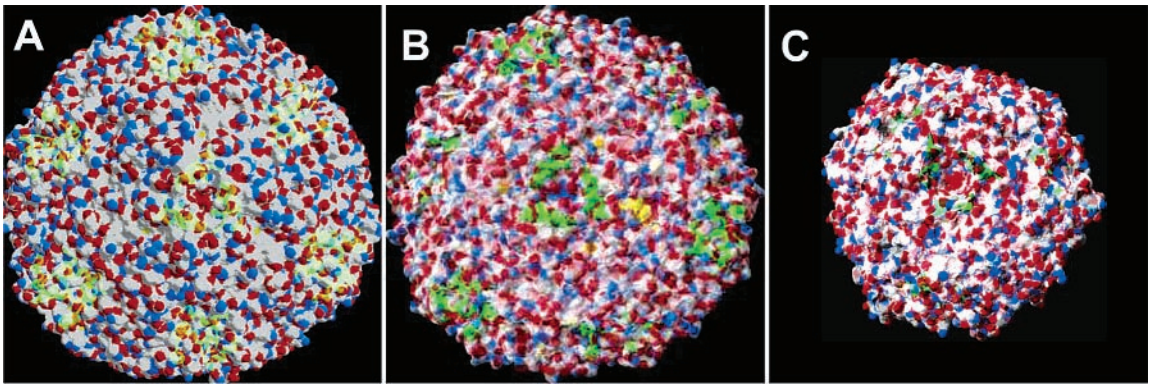

FIGURE 3. Electrostatic potentials of maxi- and mini-ferritins—global view from the outside pores at the junction of subunit triples: (A) vertebrate maxi-ferritin (human H protein, pdb 1FHA); (B) bacterial heme-containing maxi-ferritin (*E. coli* Bfr, pdb 1BFR); (C) *Dps* mini-ferritin (*E. coli*, pdb 1DPS). Electrostatic potentials (MolMol[86]) at protein dielectric constant of 4.0, solvent dielectric constant of 80, temperature of 300 K, and ionic strength of 0.1 M are included. Surface potentials are indicated as follows:10 (red); +4 (blue). Note the acidic patches (red) at the pores.

mineral in vitro by adding a reductant and chelator; the mechanisms in vivo are not known but two current models are discussed below (see Iron OUT).

The multiple functions of ferritin related to, and possibly derived from, both di-iron catalytic and pore proteins are fitted into a unique, self-assembling, spherical ferritin structure. Nature appears to have been "tweaking" the ferritin structure using functional sites in other proteins as information sources to reach a single solution to the problem of concentrating iron to physiological levels. The iron concentrating property of the ferritins applied to trapping oxidants and protecting DNA may be a convergent biological strategy. Recent thinking about the ferritins is a shift from the older view of a rigid, relatively inactive protein-coated iron core to the contemporary view of an active, flexible, complex protein catalyst and ion translocator. Still to be solved for the ferritins are problems of protein folding, supramolecular assembly, biomineralization, redox biochemistry, and gene regulation, which have general significance for chemistry, biology, medicine, and nutrition.

Structure

Subunits. Ferritin protein cages self-assemble from 24 subunits that are four-helix bundles (polypeptide tetrads of α-helices) and are designated A, B, C, and D (Figure 1). In maxi-ferritins, a short fifth helix is turned at 60° to the helix-bundle axis and is the most phylogenetically variable part of the sequence. Ferritin subunits are catalytically (F_{ox}) active (H-type) except in animals where a second ferritin encodes a catalytically inactive subunit (L-type) that co-assembles with H-types.[33] H and L designations were once thought to reflect mass differences, H (heavy) and L (light), rather than the more general property of ferroxidase activity.

Assembled Structure. Extensive helix−helix interactions occur in assembled ferritin between subunit dimers and trimers and, in maxi-ferritins, tetramers. Similar interactions also occur within the subunit helix bundles and with connecting loops of single subunits (Figures 2−4). The result is global protein stability to heat (up to 80 °C)[34] and to 6 M guanidine at neutral pH.[35] Moreover, intersubunit and intrasubunit interactions are so similar[36] that subunit dissociation and subunit unfolding usually coincide. Much more is known about the 432 packing interactions in maxi-ferritins, for example,[21,36−41] than the more recently discovered 32 packing interactions in mini-ferritins, where crystal structures are now known for *Escherichia coli*,[42] *Listeria innocua*,[4] *Helicobacter pylorii*,[5] *Bacillus anthracis*,[43] *Agrobacterium tumifaciens*,[6] and *Strep-*

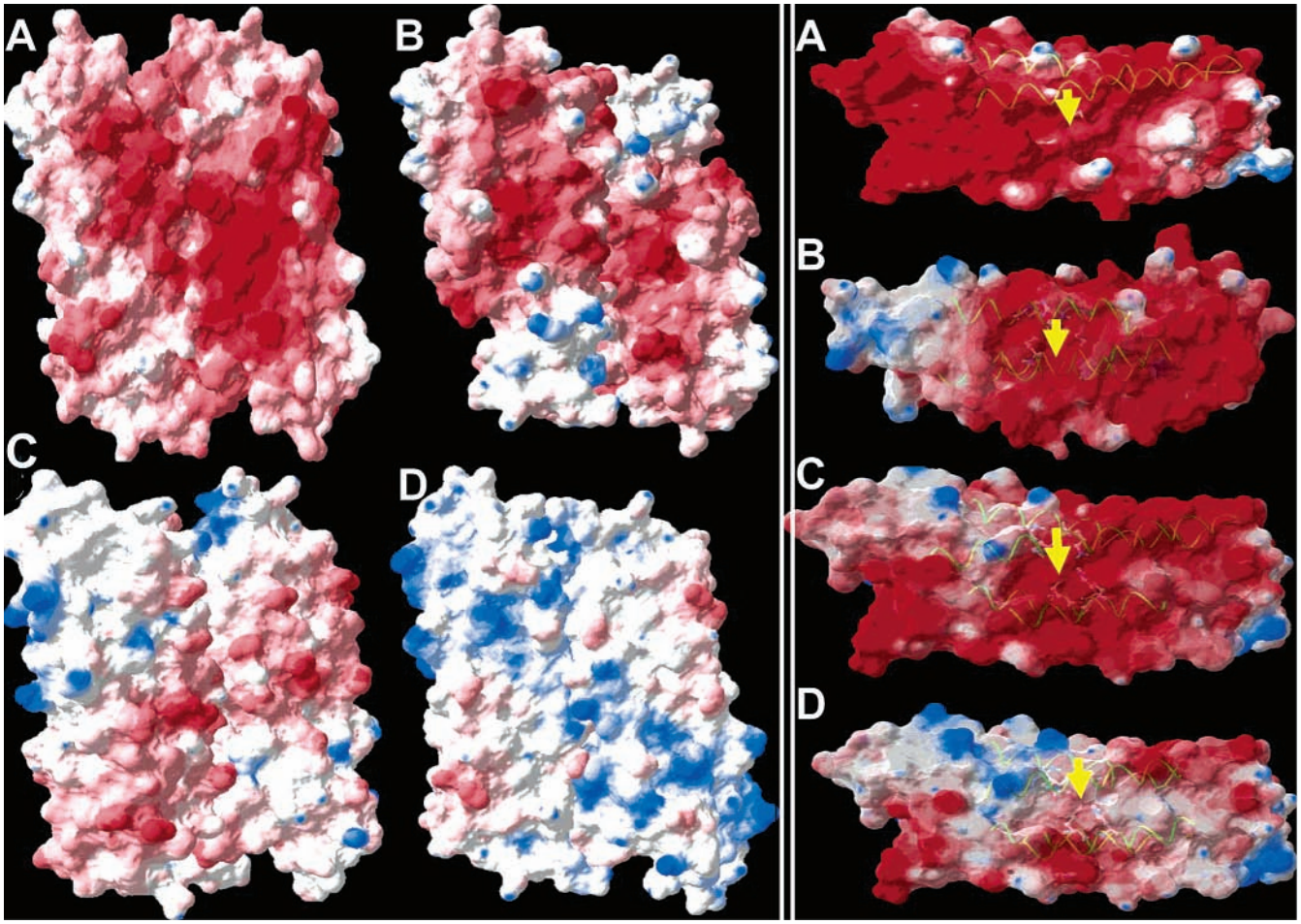

FIGURE 4. Differences in electrostatic potential (EP) distribution around nucleation sites and ferroxidase in catalytically active, inactive and chimeric maxi-ferritins. Electrostatic analyses of the charge distribution in the ferritin subunit dimer, facing the mineralization cavity (left panel) and around the intrasubunit ferroxidase (di-iron coupling/oxidation) sites in maxi-ferritins shown from a side view of the subunit interior (right panel) are presented. Frog ferritins were used as the model since data are available for both catalytically inactive (L) and active (H/M) types of subunits. (Electrostatic potential maps obtained with horse L (pdb 1DAT), mouse L (pdb 1H96), and human H (pdb 1FHA) showed the same subunit-dependent, conserved patterns of EP distribution as frog subunits). The EP analysis was performed using MolMol,[86] with the following settings: protein dielectric constant = 4.0, solvent dielectric constant = 80, T = 300 K, ionic strength = 0.2 M. All residues are included in the calculation to illustrate different paths the iron atoms take either to ferroxidase site in H-type ferritins or directly to the mineral surface in ferroxidase inactive L ferritins that are located around subunit dimer interface facing inner cavity. The surface electrostatic potential distribution was plotted on a scale from −8 to +4 for the dimer inner surface (left) and −4 to +3 for the ferroxidase site (right). In the left panel, the following are shown: (A,B) catalytically active; (C,D) catalytically inactive; (A) bullfrog M ferritin (pdb 1MFR); (B) bullfrog H ferritin (pdb 1BG7); (C) bullfrog L ferritin (pdb 1RCD); (D) nucleation site mutant of bullfrog L ferritin (E57A/E58A/E59A/E61A; pdb 1RCE). In the right panel, the following are shown: (A−C) catalytically active; (D) catalytically inactive; (A) M (H′) ferritin (pdb 1MFR); (B) H ferritin (pdb 1BG7); (C) chimeric L (K23E/Q103E/S137Q/T140D) ferritin;[22] (D) L ferritin (pdb 1RCD); green ribbon = subunit helices. (In the subunit representation of F_{ox} sites (right panel), the pores are on the right and the cavity is at the top; the yellow arrow indicates the ferroxidase site). Parts A−D in each panel correspond to decreasing rates of mineralization (left) or ferroxidation (right).

tococcus suis[7] and a predicted structure from an archaea, *Halobacterium salinarium*, is available.[44]

Bacteria with four ferritin genes,[8] such as *E. coli* (three maxi- and one mini-ferritin), appear to need different ferritins than humans, which have three known ferritin genes.[45−47] Since *E. coli*, for example, survives in a much broader range of iron and oxygen environments than humans, more ferritins may be required. On the other hand, in humans there are ∼37 ferritin sequences so far, of which ∼20 are partial or "pseudogenes",[45,46] but the possibility of more human ferritin genes to be discovered is real.

Protein Pores. The unusually high global stability of assembled ferritin masked the local unfolding/folding of ferritin pores until recently.[34,39] Studies of protein dynamics reveal that folding/unfolding usually undergoes a funnel-shaped energy landscape with multiple conformational/structural transitions that enable proteins/enzymes to function at minimal energy expense. External perturbations, such as changes in temperature, solvent (chaotropes such as urea), redox, proton gradients, or modification (phosphorylation, dephosphorylation, methylation/demethylation, ligand binding, etc.), induce metastable conformations exemplified by protein catalysis, translocation,

ion channel/pore gating, endocytosis, and virus entry. In the case of ferritin, the pores, which account for 10−15% of the subunit helix content, bracketing the C/D helix turn, unfold in response to heat (40−50°C) or to chaotropes such as 1 mM urea, measured by circular dichroism, crystallography, or both, and increased rates of iron chelation (triggered by the addition of reductant)[34,39,48] (Figures 2,3). Each ferritin pore is constructed from three ferritin subunits, tripling the effect of subunit helix changes (Figure 2).

Different sets of conserved residues control ferritin pore structure for iron flow into the catalytic ferroxidase site or out of the mineral, based on the selective effects of mutagenesis in maxi-ferritins. Much needs to be learned about how Fe moves to the ferroxidase sites after entering the ferritin pores and, in the case of certain anerobe ferritins, whether the Fe entry pores are in a different location in the protein cage.[48−51] However, all types of regulated flow of ions or neutral solutes through protein channels and pores remain subjects of active research.[52,59]

Six carboxyl side chains (Asp127 and Glu130, L sequence numbering) contributed by three pore subunits create a constriction (3.3 Å) between the pore surface and the cavity that suggests a vestibule for Fe^{2+} awaiting F_{ox} site turnover. In contrast, residues deeper in the pores, such as leucine 131 and 134, influence iron movement from the iron mineral in the ferritin cavity by controlling access of reductant to the mineral. Pores at the junctions of four ferritin subunits formed by the maxi-ferritin E helix may reflect eukaryotic-specific cytoplasmic requirements absent in mini-ferritins.

Mineralization Surface and Possible Cofactors. Mineralization of iron, calcium, and silicon uses an acidic formation surface. In ferritin, the mineralization sites are formed from conserved carboxylate residues on the inner surface clustered at the dimer interfaces (Figure 4).[4,36,41,53,54] Knowledge of mechanisms of biomineralization is limited.[54] For calcium and silicon, complex interactions among cells or organelles and biopolymeric matrixes are required.[54−56] For iron in ferritin biominerals, only the ferritin protein nanocage is required, at least in vitro; the ferritin mineral formed in vitro is structurally similar to natural biominerals by a variety of spectroscopic and microscopic techniques.[57,58] However, in vivo the flow of iron to and from ferritin likely includes macromolecules to carry electrons, iron ions, and possibly protons. (Note that for each iron ion entering the mineral, ~2 protons are released,[59] which, when a large amount of ferrous ions/ferritin protein form mineral, challenge the buffering capacity of solutions, if not the cytoplasm.)

Function−Iron IN

The first detectable reaction in iron mineralization, formation of a diferric peroxo (DFP) intermediate, requires two Fe^{2+} to traverse the outer half of the ferritin protein cage (Figure 2) to reach one of the multiple F_{ox} sites, within milliseconds. DFP has been characterized using rapid freeze trapping under single turnover conditions by Mössbauer, resonance Raman, UV−vis, and extended X-ray absorption fine structure (EXAFS) spectroscopies, which show the presence of a strained 1,2-μ peroxo bridge derived from molecular oxygen and an unusually short Fe−Fe distance of 2.54 Å. The geometry of the DFP complex may explain decay to H_2O_2 with retention or reformation of the O−O bridge in H_2O_2, and diferric oxo/hydroxo mineral precursors.[16,22,23,26,60]

Mechanisms of DFP decay to diferric mineral precursors and H_2O_2 remain to be learned. Detection of multiple diferric oxo species by Mössbauer spectroscopy and their slow decay to mineral[26] suggest the existence of multiple stages in the pathway between DFP and the diferric hydroxyl and H_2O_2 products. The multiple stages in DFP decay observed complement observations of a multiphasic turnover of the catalytic sites.[16,60]

Decay of DFP to H_2O_2 and the diferric oxy mineral precursors released from the F_{ox} sites[18,22,26,29,61] contrasts with di-iron oxygenases, where iron is retained as an active site cofactor.[25,28] The potential for reactions between DFP products, such as H_2O_2, and substrates, such as Fe^{2+}, is high in ferritin, unless they are separated by the protein during turnover. Low and nonstoichiometric radical production during ferroxidase activity indicates successful separation of substrate and products.[62] Moreover, active site regeneration rates appear to be cooperative,[16,60] likely reflecting the substrate/product channeling required to minimize reactions of substrate and product.

The two iron binding/oxidation sites in maxi-ferritins, sites A and B, were recently directly identified using protein chimeras with catalytically inactive L ferritin as the host.[23] Previous studies relied on cocrystals with ferrous analogues (Ca or Mg)[21,38] where the metal−metal distances were much longer than iron−iron distances for DFP in solution EXAFS.[22] Site A for DFP formation is the canonical E, ExxH motif common to di-iron cofactor proteins,[24] while site B is E, QxxD and ferritin-specific. (A study of Fe and Zn cocrystals of *E. coli* FTNa reported diferric sites that also bound Zn(II) in a similar configuration,[40] suggesting that the sites diverge structurally from the diferric peroxo eukaryotic maxi-ferritin site.) In the chimeric ferritin, proteins with site A alone had no ferroxidase activity. Site A and site B with either E, QxxD, or Q, QxxD formed DFP, but only with E, QxxD, was the K_{app} and Hill coefficient equivalent to catalytically active wild-type ferritin.[23] Natural variations occur among maxi-ferritins at site B, D ($RCOOH$), S (RCH_2OH), or A (RCH_3),[47,63] each with different di-iron oxidation kinetics.[23,64]

The paths taken by ferrous ions to the catalytic sites and by the catalytic products (diferric oxy mineral precursors) to the mineralization cavity are not well understood in maxi-ferritins and even less understood in mini-ferritins.[3,4,7,43,65] Negative charges from the outer surface to the cavity (see the surface potential analyses of maxi- and mini-ferritins in Figure 3), likely outline boundaries of the iron paths (Figures 3 and 4, left). Differences in the average electropotential distribution around the active site suggest that iron entering the pores would be directed to the active site in catalytically active ferritins and away from

the subunit interior toward the cavity in catalytically inactive ferritins (Figure 4, right). Changing the charge at the dimer interface had a major effect on mineralization in ferritins without a catalytic site (see Figure 4C,D, left, and ref 66) but not in a ferritin with a catalytic site.[67]

Iron OUT

Pores at the Junction of Three Subunits. Two models, not mutually exclusive, are proposed for recovering ferritin iron in vivo. In model 1, derived from experiments in cells with massive iron concentrations, cytoplasmic ferritin is incorporated into the lysosome, followed by protein degradation, iron mineral dissolution, and iron export to the cytoplasm.[68] Questions to be answered for model 1 are as follows: How does ferritin, which lacks a lysosomal transport signal, enter lysosomes? Is the ferritin mineral soluble at lysosomal pH? How does iron cross the lysosome membrane? Since, at the high iron concentrations studied, ferritin stabilizes lysosomes and protects lysosomes from oxidative damage,[69] how would lysosome ferritin degradation be beneficial? Model 2 is based on the conservation of ferritin pores that reversibly unfold/fold with small changes in temperature or millimolar urea and have the sole detectable function of increasing rates of mineral reduction/chelation and removal in vitro.[34,39,48] Ferritin pores have been characterized by X-ray crystallography, site-directed mutagenesis, and CD-spectroscopy. Questions to be answered for Model 2 are as follows: What is the pore unfolding partner in cells? How is the ferritin mineral reduced and the iron transported in cells?

The gated pores in ferritin are formed from six helices, two each contributed by three subunits (Figure 2), and are analogous to protein pores that form from polypeptide helices in cell membranes that share with ferritin pores the function of controlling ion flow.[70−77] While some pores are integral to a supramolecular structure, some result from the fusion of two supramolecular assemblies illustrated by viruses and bacterial toxins, which recruit membrane protein and create new pores. The relationship between pore structure and iron removal rates in ferritin was revealed in a mutant with selective unfolding of the pores (crystallography) and 30-fold rate increase in iron removal.[39] A set of conserved residues, identified by high conservation, proximity to the pore in three-dimensional space, no assigned function, and increasing mineral chelation rates when modified by amino acid substitution, define the pore gates as an interhelix (C−D) leucine−leucine pair, an interloop (C/D−B/C) aspartate−asparagine ion pair, and a short C−D loop.[48] Rate changes were greater for nonconservative than for conservative substitutions. The pore structure is remarkably sensitive to small changes such as shortening an amino acid side chain by a single ethylene group.

Selective destabilization of the ferritin pore structure, observed by crystallography and by rate changes in Fe removal by mutation or millimolar urea or guanidine,[34,39,48] was confirmed with CD spectroscopy where pore melting at 56 °C was lowered to physiological ranges by millimolar urea or mutation;[34] global melting is at >80 °C. Cooling, based on decreased rates of iron removal, closed pores in both wild-type ferritins and pore mutants. Ferritin iron reduction/chelation rates were linear over the range 283−313 K in Arrhenius plots (ln υ_t vs $1/T$; slope $= -E_a/R$, where E_a is the activation energy and R is the gas constant). $E =$ 88.6 and 83.5 kJ/mol for mutant pore gates and wild-type pore gates, respectively (Liu, Jin, and Theil, unpublished observations). Thus, in the iron removal assay, where concentrations of ferritin protein, reduced nicotinamide adenine dinucleotide (NADH)/flavin mononucleotide (FMN), and iron chelator are constant, the protein pore structure controls rates of ferritin iron removal. The ferritin pore structure, which can be changed independently of global ferritin structure, F_{ox} rates, or mineralization rates[34,39,48] and is phylogenetically conserved, appears to control exposure of the mineral to reductant and chelator. Under physiological conditions (37 °C, 1.7−8.3 mM urea), ferritin pores are partly unfolded.[34] In renal cells, where urea concentrations are 300−600 mM, cell-specific ferritin pore closing or controlled distribution of reductants is predicted.

Little or no iron is removed from the ferritin mineral without reductant. When different reductants are analyzed with the same chelator, the effect is much smaller than effects of changing pore structure.[34] Rates of reduction/chelation of ferritin iron were relatively similar for cysteine, ascorbate, and glutathione compared to the more efficient reduced flavins.[78,79] For a variety of reduced flavins, immobilization on a polymeric matrix inhibited the ferritin iron mineral reduction,[80] suggesting electron transfer at the mineral surface exposed by the pore.[81] Binding of flavin to ferritin protein is weak, and flavin is rarely free in cells, suggesting that in vivo a specific flavoprotein exists that binds near ferritin protein pores and reacts with the mineral with rates dependent on pore opening and mineral exposure.[78] Differences in ferritin pore dynamics can also explain differences in the hierarchy of rates of transport of small molecules though the ferritin protein cage and into the ferritin cavity.[77]

Recognition of ferritin pores by a flavoprotein complex, a protein that alters the dynamics of pore unfolding in response to cell signals, or both[82−84] can explain the phylogenetic conservation of the three-dimensional pore structure in ferritin, which in higher plants and animals extends to amino acid sequence.

Perspective

Ferritins, a family of supramolecular proteins with unique iron mineralization properties and other functions shared with both pore proteins and di-iron carboxylate proteins, have been probed with Mössbauer, EXAFS, resonance Raman and UV−vis spectroscopies that were coupled with rapid-mixing kinetics, molecular substitutions through protein engineering, and crystallization to sort the multiple metal sites into groups that are ferritin-specific and groups that are shared with other proteins. Recent results

have transformed understanding of the ferritins from a rock inside a sturdy, single-sized protein coat to an iron biomineralization reactor created from a flexible, dynamic protein cage of at least two sizes (maxi- and mini-) studded with catalytic sites and gated pores that control vectorial flow of iron, dioxygen, H_2O_2, and protons. Ferritins are the only biological molecules that control the phase transition of iron between solution and solid, using oxygen to concentrate iron for the biosynthesis of proteins in respiration (hemoglobin), photosynthesis (ferredoxins), nitrogen fixation (nitrogenase), or DNA synthesis (ribonucleotide reductase). Bacterial mini-ferritins, also called *Dps* proteins, vary the ferritin reactions by using iron to trap oxidants that damage DNA.

The striking image of ferritins as stable protein coats encasing mineral cores obscured relationships between ferritins and other proteins that share one of the multiple ferritin functions, until recently. Genomics and rapid freeze-quench kinetics revealed kinship between the ferritins and the di-iron carboxylate family of proteins,[22,23,25,26,28−30,61] while solution kinetics, combined with crystallography and protein engineering, revealed the relationships between ferritin and gated pore proteins.[34,39,48,77] Flexible local regions in the context of stable ferritin structure,[34,36,38−40] multiple types of functional sites, and multiple roles of sites such as those for iron entry and exit are all packed into the spherical, cage-like protein structure for cooperative binding of iron and oxygen, bidirectional channeling of reaction products (mineral precursors to the cavity and H_2O_2 to the protein exterior[18]), and flow of mineral reductants and chelators. Questions shared by the ferritins with other proteins, which remain to be answered include the following: What are the precise relationships of metal binding site structure to catalysis, pore function, and substrate/product channeling? Questions unique to the ferritins which remain unanswered are: What is the information for assembling the protein nanocage and cavity? Why does regulation of ferritin biosynthesis rates need both DNA and mRNA controls? What are the regulators/donors of electrons and protons to the iron mineral? How can chemists exploit the spherical ferritin protein cage structure for new drugs and for novel materials? The recent awareness of ferritins as a family of flexible, multifunctional protein cages with nanocavities present throughout biology ensures that exciting insights will come from future studies on the ferritins and Fe/O_2 chemistry in biology.

Partial support was provided by Grant NIH-DK-20251 and Cooley's Anemia Foundation.

References

(1) Theil, E. C. Ferritin. In *Handbook of Metalloproteins*; Messerschmidt, A., Huber, R., Poulos, T., Wieghardt, K., Eds.; John Wiley & Sons: Chichester, U.K., 2001; pp 771−781.

(2) Ferreira, F.; Bucchini, D.; Martin, M. E.; Levi, S.; Arosio, P.; Grandchamp, B.; Beaumont, C. Early Embryonic Lethality of H Ferritin Gene Deletion in Mice. *J. Biol. Chem.* **2000**, *275*, 3021−3024.

(3) Zhao, G.; Ceci, P.; Ilari, A.; Giangiacomo, L.; Laue, T. M.; Chiancone, E.; Chasteen, N. D. Iron and Hydrogen Peroxide Detoxification Properties of DNA-Binding Protein from Starved Cells. A Ferritin-Like DNA-Binding Protein of *Escherichia coli*. *J. Biol. Chem.* **2002**, *277*, 27689−27696.

(4) Ilari, A.; Stefanini, S.; Chiancone, E.; Tsernoglou, D. The Dodecameric Ferritin from *Listeria innocua* Contains a Novel Intersubunit Iron-Binding Site. *Nat. Struct. Biol.* **2000**, *7*, 38−43.

(5) Zanotti, G.; Papinutto, E.; Dundon, W.; Battistutta, R.; Seveso, M.; Giudice, G.; Rappuoli, R.; Montecucco, C. Structure of the Neutrophil-Activating Protein from Helicobacter Pylori. *J. Biol. Chem.* **2002**, *323*, 125−130.

(6) Ceci, P.; Ilari, A.; Falvo, E.; Chiancone, E. The Dps Protein of *Agrobacterium tumefaciens* Does Not Bind to DNA but Protects It toward Oxidative Cleavage: X-ray Crystal Structure, Iron Binding, and Hydroxyl-Radical Scavenging Properties. *J. Biol. Chem.* **2003**, *278*, 20319−20326.

(7) Kauko, A.; Haataja, S.; Pulliainen, A. T.; Finne, J.; Papageorgiou, A. C. Crystal Structure of *Streptococcus suis Dps*-Like Peroxide Resistance Protein Dpr: Implications for Iron Incorporation. *J. Mol. Chem.* **2004**, *338*, 547−558.

(8) Andrews, S. C.; Robinson, A. K.; Rodriguez-Quinones, F. Bacterial Iron Homeostasis. *FEMS Microbiol. Rev.* **2003**, *27*, 215−237.

(9) Touati, D.; Jacques, M.; Tardat, B.; Bauchard, L.; Despied, S. Lethal Oxidative Damage and Mutagenesis Are Generated by Iron in D*fur* Mutants of *Escherichia coli*: Protective Role of Superoxide Dismutase. *J. Bacteriol.* **1995**, *177*, 2305−2314.

(10) Kato, J.; Fujikawa, K.; Kanda, M.; Fukuda, N.; Sasaki, K.; Takayama, T.; Kobune, M.; Takada, K.; Takimoto, R.; Hamada, H.; Ikeda, T.; Niitsu, Y. A Mutation, in the Iron-Responsive Element of H Ferritin mRNA, Causing Autosomal Dominant Iron Overload. *Am. J. Hum. Genet.* **2001**, *69*, 191−197.

(11) Curtis, A. R.; Fey, C.; Morris, C. M.; Bindoff, L. A.; Ince, P. G.; Chinnery, P. F.; Coulthard, A.; Jackson, M. J.; Jackson, A. P.; McHale, D. P.; Hay, D.; Barker, W. A.; Markham, A. F.; Bates, D.; Curtis, A.; Burn, J. Mutation in the Gene Encoding Ferritin Light Polypeptide Causes Dominant Adult-Onset Basal Ganglia Disease. *Nat. Genet.* **2001**, *28*, 350−354.

(12) Grabill, C.; Silva, A. C.; Smith, S. S.; Koretsky, A. P.; Rouault, T. A. MRI Detection of Ferritin Iron Overload and Associated Neuronal Pathology in Iron Regulatory Protein-2 Knockout Mice. *Brain Res.* **2003**, *971*, 95−106.

(13) Beard, J. L.; Connor, J. R. Iron Status and Neural Functioning. *Annu. Rev. Nutr.* **2003**, *23*, 41−58.

(14) Torti, F. M.; Torti, S. V. Regulation of Ferritin Genes and Protein. *Blood* **2002**, *99*, 3505−3516.

(15) Theil, E. C.; Eisenstein, R. S. Combinatorial mRNA Regulation: Iron Regulatory Proteins and Iso-Iron Responsive Elements (Iso-IREs). *J. Biol. Chem.* **2000**, *275*, 40659−40662.

(16) Waldo, G. S.; Theil, E. C. Formation of Iron(III)-Tyrosinate Is the Fastest Reaction Observed in Ferritin. *Biochemistry* **1993**, *32*, 13262−13269.

(17) Sun, S.; Arosio, P.; Levi, S.; Chasteen, N. D. Ferroxidase Kinetics of Human Liver Apoferritin, Recombinant H−Chain Apoferritin, and Site-Directed Mutants. *Biochemistry* **1993**, *32*, 9362−9369.

(18) Jameson, G. N. L.; Jin, W.; Krebs, C.; Perreira, A. S.; Tavares, P.; Liu, X.; Theil, E. C.; Huynh, B. H. Stoichiometric Production of Hydrogen Peroxide and Parallel Formation of Ferric Multimers through Decay of the Diferric-Peroxo Complex, the First Detectable Intermediate in Ferritin Mineralization. *Biochemistry* **2002**, *41*, 13435−13443.

(19) The absence of μ-oxo bridges in the diferric oxy product of DFP decay, by resonance Raman spectroscopy (P. Moenne-Loccoz, personal communication), suggests hydroxy bridges.

(20) Cozzi, A.; Corsi, B.; Levi, S.; Santambrogio, P.; Biasiotto, G.; Arosio, P. Analysis of the Biologic Functions of H- and L-Ferritins in HeLa Cells by Transfection with SiRNAs and cDNAs: Evidence for a Proliferative Role of L-Ferritin. *Blood* **2004**, *103*, 2377−2383.

(21) Ha, Y.; Shi, D.; Small, G. W.; Theil, E. C.; Allewell, N. M. Crystal Structure of Bullfrog M Ferritin at 2.8 A Resolution: Analysis of Subunit Interactions and the Binuclear Metal Center. *J. Biol. Inorg. Chem.* **1999**, *4*, 243−256.

(22) Hwang, J.; Krebs, C.; Huynh, B. H.; Edmondson, D. E.; Theil, E. C.; Penner-Hahn, J. E. A Short Fe−Fe Distance in Peroxodiferric Ferritin: Control of Fe Substrate Versus Cofactor Decay? *Science* **2000**, *287*, 122−125.

(23) Liu, X.; Theil, E. C. Ferritin Reactions: Direct Identification of the Site for the Diferric Peroxide Reaction Intermediate. *Proc. Natl. Acad. Sci. U.S.A.* **2004**, *101*, 8557−8562.

(24) Nordlund, P.; Eklund, H. Di-Iron-Carboxylate Proteins. *Curr. Opin. Struct. Biol.* **1995**, *5*, 758−766.

(25) Shu, L.; Nesheim, J. C.; Kauffmann, K.; Munck, E.; Lipscomb, J. D.; Que, L., Jr. An Fe2IVO2 Diamond Core Structure for the Key Intermediate Q of Methane Monooxygenase. *Science* **1997**, *275*, 515−518.

(26) Pereira, A.; Small, G. S.; Krebs, C.; Tavares, P.; Edmondson, D. E.; Theil, E. C.; Huynh, B. H. Direct Spectroscopic and Kinetic Evidence for the Involvement of a Peroxodiferric Intermediate During the Ferroxidase Reaction in Fast Ferritin Mineralization. *Biochemistry* **1998**, *37*, 9871−9876.

(27) Moenne-Loccoz, P.; Baldwin, J.; Ley, B. A.; Loehr, T. M.; Bollinger, J. M., Jr. O_2 Activation by Non-Heme Diiron Proteins: Identification of a Symmetric Mu-1,2-Peroxide in a Mutant of Ribonucleotide Reductase. *Biochemistry* **1998**, *37*, 14659−14663.

(28) Broadwater, J. A.; Ai, J.; Loehr, T. M.; Sanders-Loehr, J.; Fox, B. G. Peroxodiferric Intermediate of Stearoyl-Acyl Carrier Protein Delta 9 Desaturase: Oxidase Reactivity During Single Turnover and Implications for the Mechanism of Desaturation. *Biochemistry* **1998**, *37*, 14664−14671.

(29) Moënne-Loccoz, P.; Krebs, C.; Herlihy, K.; Edmondson, D. E.; Theil, E. C.; Huynh, B. H.; Loehr, T. M. The Ferroxidase Reaction of Ferritin Reveals a Diferric Mu-1,2 Bridging Peroxide Intermediate in Common with Other O_2−Activating Non-Heme Diiron Proteins. *Biochemistry* **1999**, *38*, 5290−5295.

(30) Baldwin, J.; Krebs, C.; SaLeh, L.; Stelling, M.; Huynh, B. H.; Bolllinger, M., Jr.; Riggs-Gelasco, P. Structural Characterization of the Peroxodiiron(III) Intermediate Generated During Oxygen Activation by the W48A/D84E Variant of Ribonucleotide Reductase Protein R2 from *Escherichia coli*. *Biochemistry* **2003**, *42*, 13269−13279.

(31) Stubbe, J. Di-Iron-Tyrosyl Radical Ribonucleotide Reductases. *Curr. Opin. Chem. Biol.* **2003**, *7*, 183−188.

(32) Baaghil, S.; Lewin, A.; Moore, G. R.; Le Brun, N. E. Core Formation in *Escherichia coli* Bacterioferritin Requires a Functional Ferroxidase Center. *Biochemistry* **2003**, *42*, 14047−14056.

(33) Otsuka, S.; Listowsky, I.; Niitsu, Y.; Urushizaki, I. Assembly of Intra- and Interspecies Hybrid Apoferritins. *J. Biol. Chem.* **1980**, *255*, 6234−6237.

(34) Liu, X.; Jin, W.; Theil, E. C. Opening Protein Pores with Chaotropes Enhances Fe Reduction and Chelation of Fe from the Ferritin Biomineral. *Proc. Natl. Acad. Sci. U.S.A.* **2003**, *100*, 3653−3658 (Cover).

(35) Listowsky, I.; Blauer, G.; Enlard, S.; Betheil, J. J. Denaturation of Horse Spleen Ferritin in Aqueous Guanidinium Chloride Solutions. *Biochemistry* **1972**, *11*, 2176−2182.

(36) Trikha, J.; Theil, E. C.; Allewell, N. M. High-Resolution Crystal Structures of Amphibian Red-Cell L Ferritin: Potential Roles for Structural Plasticity and Solvation in Function. *J. Mol. Biol.* **1995**, *248*, 949−967.

(37) Banyard, S. H.; Stammers, D. K.; Harrison, P. M. Electron Density Map of Apoferritin at 2.8-Å Resolution. *Nature* **1978**, *271*, 282−284.

(38) Hempstead, P. D.; Yewdall, S. J.; Fernie, A. R.; Lawson, D. M.; Artymiuk, P. J.; Rice, D. W.; Ford, G. C.; Harrison, P. M. Comparison of the Three-Dimensional Structures of Recombinant Human H and Horse L Ferritins at High Resolution. *J. Mol. Biol.* **1997**, *268*, 424−448.

(39) Takagi, H.; Shi, D.; Hall, Y.; Allewell, N. M.; Theil, E. C. Localized Unfolding at the Junction of Three Ferritin Subunits. A Mechanism for Iron Release? *J. Biol. Chem.* **1998**, *273*, 18685−18688.

(40) Stillman, T. J.; Hempstead, P. D.; Artymiuk, P. J.; Andrews, S. C.; Hudson, A. J.; Treffry, A.; Guest, J. R.; Harrison, P. M. The High-Resolution X-ray Crystallographic Structure of the Ferritin (EcFtnA) of *Escherichia coli*; Comparison with Human H Ferritin (HuHF) and the Structures of the Fe(3+) and Zn(2+) Derivatives. *J. Mol. Biol.* **2001**, *307*, 587−603.

(41) Granier, T.; Langlois d'Estaintot, B.; Gallois, B.; Chevalier, J. M.; Precigoux, G.; Santambrogio, P.; Arosio, P. Structural Description of the Active Sites of Mouse L-Chain Ferritin at 1.2 A Resolution. *J. Biol. Inorg. Chem.* **2003**, *8*, 105−111.

(42) Grant, R. A.; Filman, D. J.; Finkel, S. E.; Kolter, R.; Hogle, J. M. The Crystal Structure of Dps, a Ferritin Homologue That Binds and Protects DNA. *Nat. Struct. Biol.* **1998**, *5*, 294−303.

(43) Papinutto, E.; Dundon, W. G.; Pitulis, N.; Battistutta, R.; Montecucco, C.; Zanotti, G. Structure of Two Iron-Binding Proteins from *Bacillus anthracis*. *J. Biol. Chem.* **2002**, *277*, 15093−15098.

(44) Reindel, S.; Anemuller, S.; Sawaryn, A.; Matzanke, B. F. The DpsA-Homologue of the Archaeon *Halobacterium salinarum* is a Ferritin. *Biochim. Biophys. Acta* **2002**, *1598*, 140−146.

(45) Costanzo, F.; Santoro, C.; Colantuoni, V.; Bensi, G.; Raugei, G.; Romano, V.; Cortese, R. Cloning and Sequencing of a Full Length cDNA Coding for a Human Apoferritin H Chain: Evidence for a Multigene Family. *EMBO J.* **1984**, *3*, 23−27.

(46) Santoro, C.; Marone, M.; Ferrone, M.; Costanzo, F.; Colombo, M.; Minganti, C.; Cortese, R.; Silengo, L. Cloning of the Gene Coding for Human L Apoferritin. *Nucleic Acids Res.* **1986**, *14*, 2863−2876.

(47) Levi, S.; Corsi, B.; Bosisio, M.; Invernizzi, R.; Volz, A.; Sanford, D.; Arosio, P.; Drysdale, J. A. Human Mitochondrial Ferritin Encoded by an Intronless Gene. *J. Biol. Chem.* **2001**, *276*, 24437−24440.

(48) Jin, W.; Takagi, H.; Pancorbo, N. M.; Theil, E. C. "Opening" the Ferritin Pore for Iron Release by Mutation of Conserved Amino Acids at Interhelix and Loop Sites. *Biochemistry* **2001**, *40*, 7525−7532.

(49) Macedo, S.; Romao, C. V.; Mitchell, E.; Matias, P. M.; Liu, M. Y.; Xavier, A. V.; LeGall, J.; Teixeira, M.; Lindley, P.; Carrondo, M. A. The Nature of the Di-Iron Site in the Bacterioferritin from *Desulfovibrio desulfuricans*. *Nat. Struct. Biol.* **2003**, *10*, 285−290.

(50) Levi, S.; Luzzago, A.; Cesareni, G.; Cozzi, A.; Franceschinelli, F.; Albertini, A.; Arosio, P. Mechanism of Ferritin Iron Uptake: Activity of the H−Chain and Deletion Mapping of the Ferro-Oxidase Site. *J. Biol. Chem.* **1988**, *263*, 18086−18092.

(51) Treffry, A.; Bauminger, E. R.; Hechel, D.; Hodson, N. W.; Nowik, I.; Yewdall, S. J.; Harrison, P. M. Defining the Roles of the Threefold Channels in Iron Uptake, Iron Oxidation and Iron-Core Formation in Ferritin: A Study Aided by Site-Directed Mutagenesis. *Biochem. J.* **1993**, *296*, 721−728.

(52) Lee, J. K.; Khademi, S.; Harries, W.; Savage, D.; Miercke, L.; Stroud, R. M. Water and Glycerol Permeation through the Glycerol Channel GlpF and the Aquaporin Family. *J. Synchrotron Radiat.* **2004**, *11*, 86−88.

(53) Lawson, D. M.; Artymiuk, P. J.; Yewdall, S. J.; Smith, J. M. A.; Livingstone, J. C.; Treffry, A.; Luzzago, A.; Levi, S.; Arosio, P.; Cesareni, G.; Thomas, C. D.; Shaw, W. V.; Harrison, P. M. Solving the Structure of Human H Ferritin by Genetically Engineering Intermolecular Crystal Contacts. *Nature* **1991**, *349*, 541−544.

(54) Gotliv, B. A.; Addadi, L.; Weiner, S. Mollusk Shell Acidic Proteins: In Search of Individual Functions. *ChemBioChem* **2003**, *4*, 522−529.

(55) Komeili, A.; Vali, H.; Beveridge, T. J.; Newman, D. K. Magnetosome Vesicles Are Present before Magnetite Formation, and MamA Is Required for Their Activation. *Proc. Natl. Acad. Sci. U.S.A.* **2004**, *101*, 3839−3844.

(56) Weiner, S.; Addadi, L. Biomineralization. At the Cutting Edge. *Science* **2002**, *298*, 375−376.

(57) Theil, E. C. Ferritin: Structure, Gene Regulation, and Cellular Function in Animals, Plants, and Microorganisms. *Annu. Rev. Biochem.* **1987**, *56*, 289−315.

(58) Wade, V. J.; Levi, S.; Arosio, P.; Treffry, A.; Harrison, P. M.; Mann, S. Influence of Site-Directed Modifications on the Formation of Iron Cores in Ferritin. *J. Mol. Biol.* **1991**, *221*, 1443−1452.

(59) Chasteen, N. D.; Harrison, P. M. Mineralization in Ferritin: An Efficient Means of Iron Storage. *J. Struct. Biol.* **1999**, *126*, 182−194.

(60) Treffry, A.; Zhao, Z.; Quail, M. A.; Guest, J. R.; Harrison, P. M. Iron (II) Oxidation by H Chain Ferritin: Evidence from Site-Directed Mutagenesis that a Transient Blue Species is Formed at the Dinuclear Iron Center. *Biochemistry* **1995**, *34*, 15204−15213.

(61) Bou-Abdallah, F.; Papaefthymiou, G. C.; Scheswohl, D. M.; Stanga, S. D.; Arosio, P.; Chasteen, N. D. μ-1,2-Peroxobridged Di-Iron(III) Dimer Formation in Human H−Chain Ferritin. *Biochem. J.* **2002**, *364*, 57−63.

(62) Chen-Barrett, Y.; Harrison, P. M.; Treffry, A.; Quail, M. A.; Arosio, P.; Santambrogio, P.; Chasteen, N. D. Tyrosyl Radical Formation During the Oxidative Deposition of Iron in Human Apoferritin. *Biochemistry* **1995**, *34*, 7847−7853.

(63) Dickey, L. F.; Sreedharan, S.; Theil, E. C.; Didsbury, J. R.; Wang, Y.-H.; Kaufman, R. E. Differences in the Regulation of Messenger RNA for Housekeeping and Specialized-Cell Ferritin. A Comparison of Three Distinct Ferritin Complementary DNAs, the Corresponding Subunits, and Identification of the First Processed in Amphibia. *J. Biol. Chem.* **1987**, *262*, 7901−7907.

(64) Langlois d'Estaintot, B.; Santambrogio, P.; Granier, T.; Gallois, B.; Chevalier, J. M.; Precigoux, G.; Levi, S.; Arosio, P. Crystal Structure and Biochemical Properties of the Human Mitochondrial Ferritin and Its Mutant Ser144Ala. *J. Mol. Biol.* **2004**, *340*, 277−93.

(65) Yamamoto, Y.; Poole, L. B.; Hantgan, R. R.; Kamio, Y.; Grant, R. A.; Filman, D. J.; Finkel, S. E.; Kolter, R.; Hogle, J. M. An Iron-Binding Protein, Dpr, from Streptococcus Mutans Prevents Iron-Dependent Hydroxyl Radical Formation in Vitro. The Crystal Structure of Dps, a Ferritin Homologue That Binds and Protects DNA. *J. Bacteriol.* **2002**, *184*, 2931−2939.

(66) Waldo, G. S.; Theil, E. C. Ferritin and Iron Biomineralization. In *Comprehensive Supramolecular Chemistry, Bioinorganic Systems*; Suslick, K. S., Ed.; Pergamon Press: Oxford, U.K., 1996; Vol. 5, pp 65−89.

(67) Bou-Abdallah, F.; Biasiotto, G.; Arosio, P.; Chasteen, N. D. The Putative "Nucleation Site" in Human H−Chain Ferritin Is Not Required for Mineralization of the Iron Core. *Biochemistry* **2004**, *43*, 4332−4337.
(68) Radisky, D. C.; Kaplan, J. Iron in Cytosolic Ferritin Can Be Recycled through Lysosomal Degradation in Human Fibroblasts. *Biochem. J.* **1998**, *336* (Pt 1), 201−205.
(69) Persson, H. L.; Nilsson, K. J.; Brunk, U. T. Novel Cellular Defenses against Iron and Oxidation: Ferritin and Autophagocytosis Preserve Lysosomal Stability in Airway Epithelium. *Redox Rep.* **2001**, *6*, 57−63.
(70) Zhang, S.; Cunningham, K.; Collier, R. J. Anthrax Protective Antigen: Efficiency of Translocation Is Independent of the Number of Ligands Bound to the Prepore. *Biochemistry* **2004**, *43*, 6339−6343.
(71) Modis, Y.; Ogata, S.; Clements, D.; Harrison, S. C. Structure of the Dengue Virus Envelope Protein after Membrane Fusion. *Nature* **2004**, *427*, 313−319.
(72) Gibbons, D. L.; Vaney, M. C.; Roussel, A.; Vigouroux, A.; Reilly, B.; Lepault, J.; Kielian, M.; Rey, F. A. Conformational Change and Protein−Protein Interactions of the Fusion Protein of Semliki Forest Virus. *Nature* **2004**, *427*, 320−325.
(73) Kaplan, J. H. Biochemistry of Na,K−Atpase. *Annu. Rev. Biochem.* **2002**, *71*, 511−535.
(74) MacKinnon, R. Potassium Channels. *FEBS Lett.* **2003**, *555*, 62−65.
(75) Agre, P.; Kozono, D. Aquaporin Water Channels: Molecular Mechanisms for Human Diseases. *FEBS Lett.* **2003**, *555*, 72−78.
(76) Yau, S. T.; Petsev, D. N.; Thomas, B. V.; Vekilov, P. G. Molecular-Level Thermodynamic and Kinetic Parameters for the Self-Assembly of Apoferritin Molecules into Crystals. *J. Mol. Biol.* **2000**, *303*, 667−678.
(77) Yang, X.; Arosio, P.; Chasteen, N. D. 2000 Molecular Diffusion into Ferritin: Pathways, Temperature Dependence, Incubation Time, and Concentration Effects. *Biophys. J.* **2000**, *78*, 2049−2059.
(78) Sirivech, S.; Frieden, E.; Osaki, S. The Release of Iron from Horse Spleen Ferritin by Reduced Flavins. *Biochem. J.* **1974**, *143*, 311−315.
(79) Dognin, J.; Crichton, R. R. Mobilisation of Iron from Ferritin Fractions of Defined Iron Content by Biological Reductants. *FEBS Lett.* **1975**, *54*, 234−6.
(80) Jones, T.; Spencer, R.; Walsh, C. Mechanism and Kinetics of Iron Release from Ferritin by Dihydroflavins and Dihydroflavin Analogues. *Biochemistry* **1978**, *17*, 4011−4017.
(81) Jameson, G. N.; Jameson, R. F.; Linert, W. New Insights into Iron Release from Ferritin: Direct Observation of the Neurotoxin 6-Hydroxydopamine Entering Ferritin and Reaching Redox Equilibrium with the Iron Core. *Org Biomol. Chem.* **2004**, *2*, 2346−2351.
(82) Vaisman, B.; Fibach, E.; Konijn, A. M. Utilization of Intracellular Ferritin Iron for Hemoglobin Synthesis in Developing Human Erythroid Precursors. *Blood* **1997**, *90*, 831−838.
(83) Lipschitz, D. A.; Simon, M. O.; Lynch, S. R.; Dugard, J.; Bothwell, T. H.; Charlton, R. W. Some Factors Affecting the Release of Iron from Reticuloendothelial Cells. *Br. J. Haematol.* **1971**, *21*, 289−303.
(84) Peto, T. E. A.; Rutherford, T. R.; Thompson, J. L.; Weatherall, D. J. Iron Metabolism in Murine Erythroleukaemic Cells. *Br. J. Haematol.* **1983**, *54*, 623−631.
(85) Trikha, J.; Waldo, G. S.; Lewandowski, F. A.; Theil, E. C.; Weber, P. C.; Allewell, N. M. Crystallization and Structural Analysis of Bullfrog Red Cell L-Subunit Ferritins. *Proteins* **1994**, *18*, 107−118.
(86) Koradi, R.; Billeter, M.; Wuthrich, K. MOLMOL: A Program for Display and Analysis of Macromolecular Structures. *J. Mol. Graphics* **1996**, *14*, 51−55, 29−32.

AR0302336